JOURNAL OF SOLID STATE CHEMISTRY 73, 536–543 (1988)

Substitution of Ca for La Ions in the U–Ca Mixed Oxides: Effects on Thermal Stability of the Fluorite Phase

M. P. HERRERO AND R. M. ROJAS*

Instituto Química Inorgánica "Elhúyar," CSIC Serrano 113,
28006 Madrid, Spain

Received July 10, 1987; in revised form November 3, 1987

Two series (A and B) of U–Ca–La oxides have been prepared in air at 1400°C. Series A corresponds to the composition range $(U_{0.5}Ca_{0.5-y}La_y)O_{2\pm x}$, where $0 \leq y \leq 0.5$, and series B corresponds to $(U_{0.67}Ca_{0.33-y}La_y)O_{2+x}$, where $0 \leq y \leq 0.33$. The obtained products have been characterized by X-ray powder diffraction, thermal analysis, and electron microscopy. In materials belonging to series B a f.c.c. fluorite-type structure is always obtained as a single phase over the whole composition range. Thermal stability up to 1400°C is achieved when the lanthanum content in these samples ranges from $0.13 \leq y \leq 0.33$. Electron diffraction patterns show diffuse maxima indicating the existence of systematic short-range deviations from the periodicity of the average unit cell. In series A, five well-defined regions are observed, but the fluorite structure is not formed. © 1988 Academic Press, Inc.

Introduction

Compounds crystallizing with the fluorite-type structure are able to support large deviations from stoichiometry, which can be attributed to the inherent ability of the fluorite lattice to accommodate defects. Among them the fluorite oxides are an interesting class of compounds, including such examples as stabilized ZrO_2, doped Bi_2O_3, UO_2, and CeO_2, for which, and because of their anionic conductivity properties, many technological uses have been demonstrated. Recently, for example, it has been shown that nonstoichiometric oxides of the general formula $(U,M)O_{2\pm x}$ (M = Sc, Y, Pr, Dy) having the fluorite structure are good electrode materials and offer some advantages over conventional noble metals (*1–4*). In general, the introduction of lower oxidation state cations (Ca^{2+}, Mg^{2+}, Y^{3+}, and various rare-earth cations) in the host fluorite lattice leads to the obtainment of nonstoichiometric phases in which oxygen ions constitute the mobile species. Moreover varying states of order in the fluorite lattice have been found in these nonstoichiometric oxides, ranging from very small clusters and short-range order to long-range order, which can lead to the formation of new structures (*5–7*).

In earlier studies on alkaline-earth uranates, the formation of a fluorite phase has been described (*8*, *9*). More recently a reinvestigation of the phase relationship in the $CaO–UO_2$ system has been carried out (*10*) but scarce attention has been paid to the U–Ca fluorite phase (*11*). This corresponds to the $U_{0.67}Ca_{0.33}O_{2\pm x}$ composition, which can also be formulated as Ca

---

* To whom correspondence should be addressed.

0022-4596/88 $3.00

U_2O_6 (*8*) and it transforms reversibly to CaU_2O_7 in air at about 1100°C. Both CaU_2O_6 and CaU_2O_7 have been reported to be slightly nonstoichiometric (*10, 12, 13*).

On the other hand, solid-state studies on the uranium–lanthanum–oxygen system have pointed out the existence of a fluorite-type solid solution $(U, La)O_{2\pm x}$ stable over a wide composition and temperature range (*14, 15*). Bearing in mind all indicated above, we have undertaken the stabilization of fluorite phases formed in the U–*M*–O system (*M* = alkaline–earth cation), by the addition of lanthanide ions. In this paper some results obtained in the U–Ca–La–O system are described.

Experimental

Two series, A and B, of uranium–calcium–lanthanum oxides were prepared as indicated in Tables I and II, respectively, by mixing stoichiometric amounts of lanthanum uranyl propionate $LaUO_2(C_2H_5COO)_5 \cdot 3H_2O$, $CaCO_3$ (Merck reagent grade), and UO_3 (from J.E.N., Spain), except for sample A-11 which was obtained from a mixture of calcium uranyl butyrate $Ca[UO_2(C_3H_7COO)_3]_2 \cdot 7H_2O$ and $CaCO_3$ and sample B-1 which was directly prepared by decomposition of calcium uranyl carboxylate. Both carboxylates were synthesized by the usual procedure described elsewhere (*9, 16*). The two series can be considered as formally derived from calcium monouranate $CaUO_4$ (series A) or calcium diuranate (series B) by progressive substitution of calcium ions for lanthanum ions. Starting mixtures after being pyrolized at 750°C were calcined at 1400°C in air in platinum containers for 12 hr. Samples were then quenched by rapidly removing them from the furnace.

The alternative use of traditional ceramic methods implies prolonged and consecutive periods of heating and annealing that have been obviated by using the corresponding uranyl carboxylate as precursor.

TABLE I

STARTING COMPOSITION, OBTAINED PHASES, AND CALCULATED CELL PARAMETERS FOR SAMPLES CORRESPONDING TO SERIES A

Sample	Starting composition			Obtained products	Cell parameters (nm)
	U	Ca	La		
A-1	1.0	1.0	0.0	R^a	a_H = 0.3868 c_H = 1.7529
A-2	1.0	0.9	0.1	R	a_H = 0.38669(7) c_H = 1.74928(1)
A-3	1.0	0.8	0.2	$R + R_{III}{}^b$	
A-4	1.0	0.7	0.3	$R + R_{III}$	
A-5	1.0	0.6	0.4	$R + R_{III}$	
A-6	1.0	0.5	0.5	$R_{III} + R$	
A-7	1.0	0.4	0.6	$R_{III} + R$	
A-8	1.0	0.3	0.7	R_{III}	a_H = 1.56381(8) c_H = 1.8412 (1)
A-9	1.0	0.2	0.8	R_{III} + fluorite	
A-10	1.0	0.1	0.9	Fluorite + R_{III}	
A-11	1.0	0.0	1.0	Fluorite	0.5520(3) γ

[a] $CaUO_4$-type structure (*17*).

[b] Rombohedral R_{III}-type structure (*14*).

TABLE II

Composition, Obtained Phases, and Calculated Cell Parameters for Samples Corresponding to Series B

Sample	Starting composition U	Ca	La	Obtained products	Calculated composition[a]	Cell parameters *a* (nm)
B-1	1.0	0.5	0.0	Fluorite	$(U_{0.67}Ca_{0.33})O_{2.005}$	0.5371(3)
B-2	1.0	0.4	0.1	Fluorite	$(U_{0.67}Ca_{0.27}La_{0.06})O_{2.025}$	0.5394(3)
B-3	1.0	0.3	0.2	Fluorite	$(U_{0.67}Ca_{0.20}La_{0.13})O_{2.070}$	0.5414(2)
B-4	1.0	0.2	0.3	Fluorite	$(U_{0.67}Ca_{0.13}La_{0.20})O_{2.105}$	0.5437(7)
B-5	1.0	0.1	0.4	Fluorite	$(U_{0.67}Ca_{0.06}La_{0.27})O_{2.135}$	0.5457(4)
B-6	1.0	0.0	0.5	Fluorite	$(U_{0.67}La_{0.33})O_{2.175}$	0.5480(3)

[a] The oxygen content has been calculated assuming all uranium to be U(V).

X-ray powder diffraction patterns were recorded on a Siemens D-500 diffractometer with monochromatized Cu*Kα* radiation and W or Si as internal standards. Diagrams were scanned at 1/10° 2*θ* · min^{-1} and the data were refined by using a least-squares program. Thermal stability was investigated using Stanton STA 781 equipment. Runs were carried out at 10° · min^{-1} heating rate in dynamic air (50 ml · min^{-1}) up to 1400°C. Cooling curves were also registered. Electron diffraction studies were made with a Siemens Elmiskop 102 electron microscope, operated at 100 kV and fitted with a double tilting goniometer stage, allowing tilts of ±45° around both axes. Samples for study were crushed in an agate mortar and suspended in acetone, then transferred to holey carbon-coated copper grids.

Results and Discussion

Series A (*Table I*)

X-ray powder diffraction analysis reveals that the progressive substitution of lanthanum ions into the calcium monouranate lattice (A-1 sample), whose crystal structure is closely related to that of the fluorite phase (*17*), leads to the formation of five well-defined regions:

(a) When the lanthanum amount entering the lattice is La = 0.1 (A-2 sample), an *R* single phase with the $CaUO_4$ rombohedral symmetry is obtained. The calculated hexagonal cell parameters for this new phase that corresponds to the composition $UCa_{0.9}La_{0.1}O_{4\pm x}$ are a_H = 0.38669(7) nm; c_H = 1.74928(1) nm.

(b) For a lanthanum content ranging from La = 0.2 to 0.6 (A-3 to A-7 samples), a biphasic region $R + R_{III}$ is formed. As the lanthanum content increases a new phase with the R_{III} rombohedral structure described by Keller (*14*) in the U–La–O system progressively takes place.

(c) For a lanthanum content of La = 0.7 (sample A-8) the above-mentioned R_{III} rombohedral phase, with a nominal composition of $UCa_{0.3}La_{0.7}O_{4\pm x}$, is now obtained as a single phase. The calculated cell parameters are a_H = 1.56381(8) nm, c_H = 1.8412(1) nm. No phase with this structure and composition, containing both calcium and lanthanum ions within the lattice, has been previously reported.

(d) For higher lanthanum contents La = 0.8 and 0.9 (A-9 and A-10 samples) a f.c.c. fluorite phase gradually appears coexisting with the R_{III} phase.

(e) Finally, in sample A-11, in which all Ca cations have been substituted for lanthanum ions, the f.c.c. fluorite phase is ob-

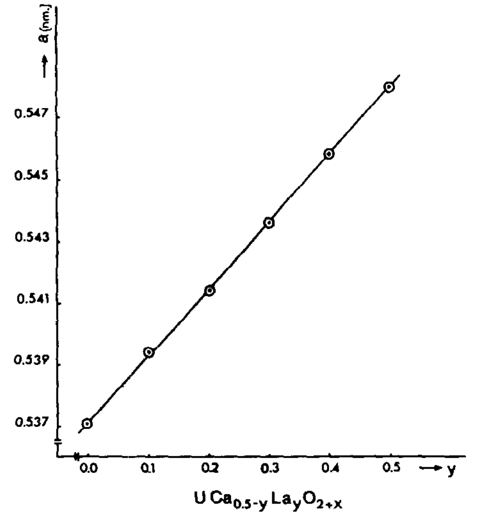

FIG. 1. Lattice parameter evolution vs lanthanum content in samples corresponding to series B.

tained, as a single phase. It corresponds to the already known composition $U_{0.5}La_{0.5}O_{2\pm x}$ (*15*). The calculated cell parameter is a = 0.5520(3) nm.

A more detailed characterization of both R and R_{III} phases formed in this series is in progress.

Series B (*Table II*)

In this series, the substitution of calcium for lanthanum ions in calcium diuranate has been made in the proportions indicated in Table II. From X-ray diffraction patterns it has been seen that f.c.c. fluorite-type structure is obtained as a single phase over the whole composition range. The cubic cell parameters, as shown in Fig. 1, increase linearly as a function of the lanthanum content.

The oxygen content of these samples has not been determined; however, a theoretical calculation has been made on the basis of all uranium being U(V) (see Table II). If all uranium was hypothesized to be U(VI) the oxygen content would be extremely high and it is not probable that the fluorite lattice could accomodate such anion excess without altering its structure. On the other hand, it is very unlikely that uranium(IV) exists in these samples because of the experimental conditions at which they have been obtained. It seems more likely that uranium(V) is the main oxidation state. This would imply hyperstoichiometric compositions.

Thermograms recorded for these samples from room temperature up to 1400°C are presented in Fig. 2. It can be observed that for sample B-1, which corresponds to an U : Ca ratio of 2 : 1 with a nominal composition of $U_{0.67}Ca_{0.33}O_{2+x}$, a progressive weight increase is observed in the temperature range 450–825°C, while in the differential thermal analysis (DTA) curve two endothermic effects accompany this weight gain. The X-ray diagram taken at this step fairly agrees with data reported for CaU_2O_7 (*13*). This compound remains stable from 825°C up to about 1100°C where a weight loss takes place, the fluorite phase being formed again. While cooling down, the fluorite phase is destroyed and a new weight increase is observed. These results agree with those previously reported (*8, 12, 18*) for the reversible transformation,

$$CaU_2O_7 \underset{\text{air}}{\overset{1100°C}{\rightleftharpoons}} CaU_2O_6 + \tfrac{1}{2} O_2,$$

although slight differences are observed between experimental and theoretical weight variations calculated according to the above indicated equation. This fact could be attributed to some deviations from stoichiometry bigger than those previously reported for both compounds (*8, 10*).

A similar behaviour is observed for sample B-2 with a lanthanum content of 0.1, although the weight gain of 2% attributed to the incorporation of oxygen into the lattice takes place in a single step at higher temperature, being the f.c.c. cubic structure partially retained. Nevertheless, the subsequent transformation into the fluorite phase takes place at almost the same temperature

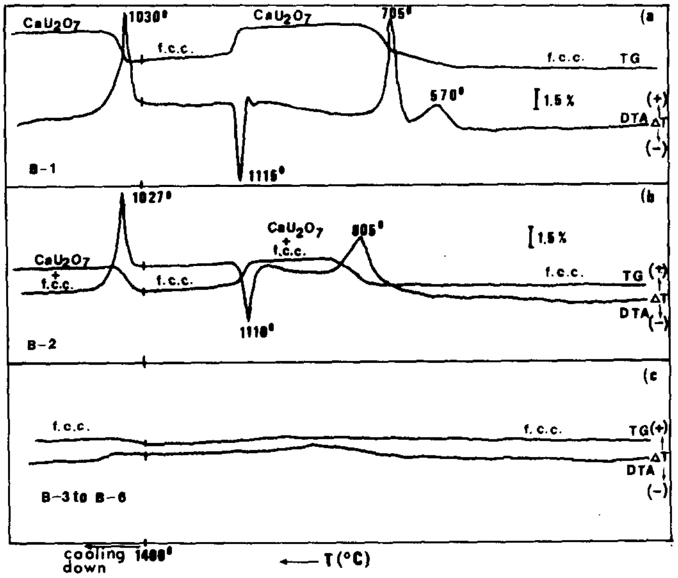

FIG. 2. DTA and TG curves recorded on samples belonging to series B (≃65 mg sample, 10 mg/full scale sensitivity).

at which it occurs for sample B-1. For all other samples no appreciable weight variations are observed in the TG curves, nor any thermal effects appear in the DTA traces. These results indicate that for samples with compositions $(U_{0.67}Ca_{0.33-y}La_y)O_{2+x}$ $(0.13 \leq y \leq 0.33)$, the fluorite-type structure is preserved over the whole temperature range studied.

An electron diffraction study has been carried out for all samples belonging to series B, and Fig. 3 shows selected area diffraction patterns corresponding to the [011] zone axis for every sample. It can be clearly seen that in addition to the diffraction spots corresponding to the reciprocal lattice of the fluorite cell, some diffuse diffraction maxima are present in the areas in between. These additional spots always occur along the ⟨111⟩ direction, and their presence is indicative of the existence of systematic short-range deviations from the periodicity of the average unit cell (*19*). Shape, size, and number of diffuse maxima vary with the composition of the sample, i.e., with the lanthanum content. Thus, for example, when nominal composition corresponds to $U_{0.67}Ca_{0.33}O_{2+x}$, sample B-1, there exists one diffuse diffraction maxima located at $\frac{1}{2}$ ⟨111⟩. This situation is analogous for samples B-2, B-3, and B-4, although the shape changes from oval to almost circular. However, samples B-5 and B-6 show two maxima along the same ⟨111⟩ direction but located at about $\frac{1}{3}$ and $\frac{2}{3}$ ⟨111⟩ and situated on each side of the diagonal. Diffuse maxima are also present in other zone axes but they are much weaker, and so it is not yet possible to build up a complete geometric reciprocal lattice corresponding to this type of observed diffuse scattering. The image corresponding to the sample B-6 in the [011] zone axis can be seen in Fig. 4, showing irregular features in contrast.

Discussion

The observed diffuse scattering resembles, in some respects, that found in mixed

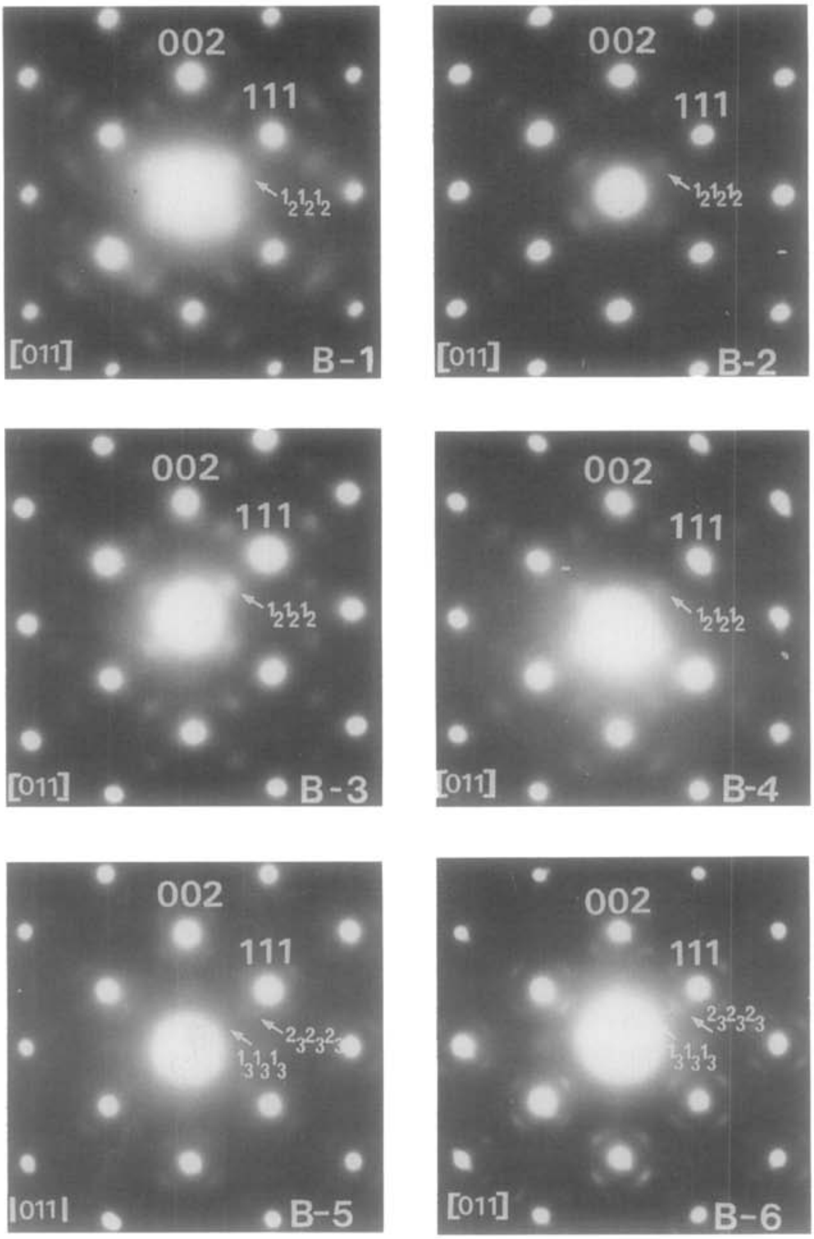

FIG. 3. Electron diffraction patterns corresponding to series B in the [011] zone axis.

oxide systems with the fluorite structure, such as $(Tb_xGd_{1-x})_2Zr_2O_{7+y}$ (*7*) and $Ca_xM_{1-x}O_{2-x}$ (M = Zr, Hf) (*20–22*), among others; it has been interpreted in terms of oxygen atoms away from their ideal fluorite positions and the formation of ordered zones or microdomains residing coherently within the cubic parent crystals. It is, however, worthwhile to mention that the diffuse maxima observed in those systems

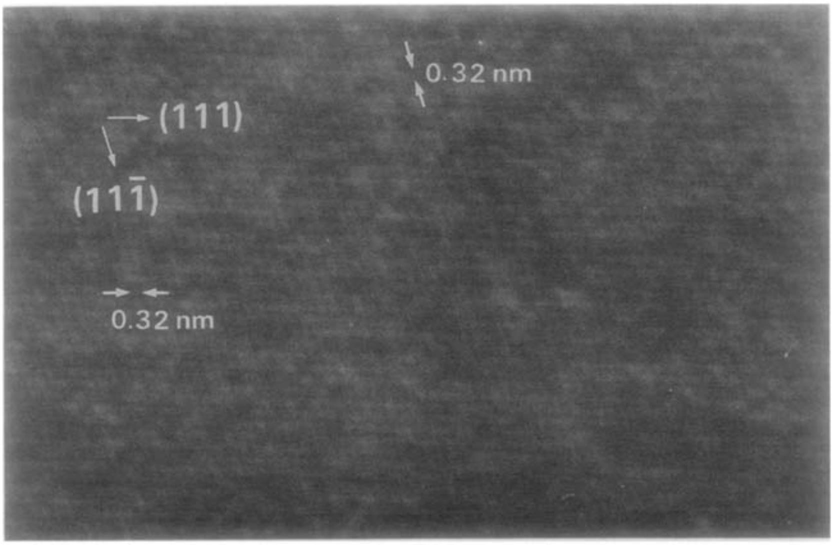

FIG. 4. Electron micrograph of the sample B-6 showing fringes corresponding to (111) planes and irregular features in contrast.

do not change their geometrical features (position, size, and form) with variation in the composition of the dopant ions, in contrast with what was observed in our own results. This fact could be indicative of a different kind of short-range interaction in the U–Ca–La–O system. A prolonged annealing of samples in the above-mentioned systems gave place to an entirely ordered structure with sharp spots which lay in positions that were occupied by diffuse maxima in patterns from disordered samples, i.e., quenched samples (*7, 20, 21*). Moreover, it is now widely accepted that nonstoichiometry on hyperstoichiometric UO_{2+x} and some other fluorite oxides is explained on the basis of cluster formation, based in dopant aggregation with two or more substitutional ions and their accompanying interstitial anions (*23, 24*). According to that, a likely explanation of the role of lanthanum in stabilizing the fluorite phase in the U–Ca–La mixed oxides is the formation of large defect clusters containing the rare-earth ions. Such clusters would be responsible for the short-range interactions detected in electron diffraction patterns. We intend to perform a more detailed structural study by EXAFS spectroscopy that is able to yield information on the local structural environment of individual atom types. Moreover a prolonged annealing of these samples will also probably offer some light in the elucidation of the nature of the local arrangement.

Acknowledgment

We are grateful to Mr. A. García Delgado for assistance with electron microscopy.

References

1. S. P. S. BADWALL, *J. Electroanal. Chem.* **146,** 425 (1983).
2. S. P. S. BADWALL, *J. Electroanal. Chem.* **161,** 75 (1984).
3. S. P. S. BADWALL, M. J. BANNISTER, AND M. J. MURRAY, *J. Electroanal. Chem.* **168,** 363 (1984).
4. S. P. S. BADWALL, F. T. CIACCHI, AND D. K. SOOD, *J. Mater. Sci.* **21,** 4035 (1986).
5. H. J. ROSELL, *in* "Advances in Ceramics" (A. H. Hever, Ed.), Vol. 3, pp. 47–63, Amer. Ceram. Soc., Columbus, OH (1981).

6. H. J. Rosell and H. G. Scott, *J. Phys. C* **38,** 28 (1977).
7. M. P. van Dijk, F. C. Mijlhoff, and A. J. Burggraaf, *J. Solid State Chem.* **62,** 377 (1986).
8. C. Brisi, M. Montorsi, and G. B. Acquarone, *Atti Accad. Sci. Torino Cl. Sci. Fis. Mat. Nat.* **106,** 257 (1971).
9. R. M. Rojas, V. González, J. Bermúdez, and M. L. de Paz, *Thermochim. Acta* **32,** 257 (1979).
10. J. Holc and D. Kolar, *J. Solid State Chem.* **61,** 260 (1986).
11. T. Yamashita and T. Fujino, *J. Nucl. Mater.* **136,** 117 (1985).
12. E. H. P. Cordfunke and B. O. Loopstra, *J. Inorg. Nucl. Chem.* **29,** 51 (1967).
13. C. Brisi and M. Montorsi, *Ann. Chim. (Rome)* **59,** 400 (1969).
14. H. G. Diehl and C. Keller, *J. Solid State Chem.* **3,** 621 (1971).
15. C. Keller, "MTP International Review of Science" (K. W. Bagnall, Ed.), Vol. 7, Series 2, p. 1, Butterworths, London (1975).
16. Z. M. Alikhanova and G. V. Ellert, *Russ. J. Inorg. Chem. Engl. Transl.* **16,** 63 (1971).
17. A. Prodan and F. W. Boswell, *Acta Crystallogr. Sect. B* **42,** 141 (1986).
18. H. R. Hoekstra and J. J. Katz, *J. Amer. Ceram. Soc.* **74,** 1683 (1952).
19. L. H. Schwartz and J. B. Cohen, *in* "Diffraction from Materials," Chap. 7, Academic Press, New York (1977).
20. J. G. Allpress and H. J. Rossell, *J. Solid State Chem.* **15,** 68 (1975).
21. B. Hudson and P. T. Moseley, *J. Solid State Chem.* **19,** 383 (1976).
22. H. J. Rossell, J. R. Sellar, and I. J. Wilson, "Proceedings of the XIth International Congress on Electron Microscopy," Kyoto (1986).
23. B. T. M. Willis, *Nature (London)* **197,** 755 (1963).
24. C. R. A. Catlow, A. V. Chadwick, G. N. Greaves, and L. M. Moroney, *Nature (London)* **312,** 601 (1984).